



Original article

UDK 536.425:539.25:539.531

DOI 10.17073/0368-0797-2022-8-563-572

<https://fermet.misis.ru/jour/article/view/2368>

CONTROL OF CANTOR CoCrFeMnNi HIGH-ENTROPY ALLOY MECHANICAL PROPERTIES

V. E. Gromov¹, S. V. Konovalov^{1,2}, Yu. A. Shlyarova¹,
M. O. Efimov¹, I. A. Panchenko¹

¹Siberian State Industrial University (42 Kirova Str., Novokuznetsk, Kemerovo Region – Kuzbass 654007, Russian Federation)

²Samara National Research University (34 Moskovskoe Route, Samara 443086, Russian Federation)

Abstract. The paper summarizes the research on the control of Cantor CoCrFeMnNi high-entropy alloy (HEA) mechanical properties. We studied the effects of alloying with aluminum, vanadium, manganese, titanium, silicon, carbon, and copper on the hardening of HEAs made by vacuum arc melting, laser melting, arc melting, drip casting, mechanical alloying with subsequent plasma sintering, gas sputtering followed by the shock wave and static compaction. It was shown that the addition of 2.5 % TiC and 5 % WC significantly improves the tensile strength, but reduces the elongation to failure. In the 4.4 – 155 μm grain size range, the tensile strength increases as the grain size decreases. The strength and yield limits for any grain size increase as the temperature decreases. Intensive plastic deformation forming nanoscale (~ 50 nm) grains significantly increases the tensile strength (up to 1,950 MPa) and hardness (up to 520 HV). The strength and ductility can be adjusted with subsequent isochronous and isothermal annealing. The formation of nanostructure phase states with shock compression, mechanical alloying, and subsequent spark plasma sintering significantly increase the tensile strength at room temperature while maintaining excellent plasticity (relative elongation ~ 28 %). We proposed electron-beam processing (EBP) to control the HEA mechanical properties. We analyzed the deformation curves for the HEA made by wire arc additive manufacturing after EBP at 10 – 30 J/cm² electron beam energy density and made some assumptions about the reasons for the strength and ductility decrease. We also compared the mechanical properties of Cantor alloys made by various processes and found the reasons for the spread of the strength and ductility values.

Keywords: HEA, CoCrFeMnNi, mechanical properties, alloying, structure, sintering, hardening

Funding: The research was supported by the grant of the Russian Science Foundation (project No. 20-19-00452).

For citation: Gromov V.E., Konovalov S.V., Shlyarova Yu.A., Efimov M.O., Panchenko I.A. Control of Cantor CoCrFeMnNi high-entropy alloy mechanical properties. *Izvestiya. Ferrous Metallurgy*. 2022, vol. 65, no. 8, pp. 563–572. <https://doi.org/10.17073/0368-0797-2022-8-563-572>

Оригинальная статья

УПРАВЛЕНИЕ МЕХАНИЧЕСКИМИ СВОЙСТВАМИ ВЫСОКОЭНТРОПИЙНОГО СПЛАВА CANTOR CoCrFeMnNi

В. Е. Громов¹, С. В. Коновалов^{1,2}, Ю. А. Шлярова¹,
М. О. Ефимов¹, И. А. Панченко¹

¹Сибирский государственный индустриальный университет (Россия, 654007, Кемеровская обл. – Кузбасс, Новокузнецк, ул. Кирова, 42)

²Самарский национальный исследовательский университет им. академика С.П. Королева (Россия, 443086, Самара, Московское шоссе, 34)

Аннотация. Выполнен краткий анализ работ по изменению механических свойств высокоэнтروпийного сплава (ВЭС) Cantor CoCrFeMnNi различными способами. Рассмотрено влияние легирования алюминием, ванадием, марганцем, титаном, кремнием, углеродом, медью на упрочнение ВЭС, полученного методами вакуумно-дуговой плавки, лазерной плавки, дуговой плавки и капельного литья, механического легирования с последующим плазменным спеканием, газового распыления с последующим ударно-волновым и статическим уплотнением. Показано, что добавки 2,5 % TiC и 5 % WC значительно улучшают предел прочности, но снижают относительное удлинение до разрушения. Влияние размера зерна в диапазоне 4,4 – 155 мкм заключается в увеличении

предела прочности с уменьшением размера зерна. Понижение температуры увеличивает пределы прочности и текучести для зерен всех размеров. Интенсивная пластическая деформация, формирующая наноразмерные (~50 нм) зерна, значительно увеличивает предел прочности до 1950 МПа и твердость до 520 HV. Последующие изохронные и изотермические отжиги позволяют варьировать прочность и пластичность ВЭС. Формирование наноструктурно-фазовых состояний при ударном компостировании, механическом легировании и последующем искровом плазменном спекании значительно повышает предел прочности при комнатной температуре, сохраняя отличную пластичность (относительное удлинение примерно 28 %). В качестве одного из методов модифицирования механических свойств ВЭС авторами предложена электронно-пучковая обработка (ЭПО). Выполнен анализ деформационных кривых ВЭС, полученного по технологии проволоочно-дугового аддитивного производства, после ЭПО с плотностью энергии пучка электронов 10–30 Дж/см², высказаны и обоснованы предположения о причинах снижения прочностных и пластических характеристик. Проведен сравнительный анализ механических свойств ВЭС Cantor, полученных различными методами, и отмечены причины расхождения значений прочностных и пластических параметров.

Ключевые слова: высокоэнтропийный сплав, CoCrFeMnNi, механические свойства, легирование, структура, спекание, упрочнение

Финансирование: Работа выполнена при финансовой поддержке Российского научного фонда № 20-19-00452.

Для цитирования: Громов В.Е., Коновалов С.В., Шлярова Ю.А., Ефимов М.О., Панченко И.А. Управление механическими свойствами высокоэнтропийного сплава Cantor CoCrFeMnNi // Известия вузов. Черная металлургия. 2022. Т. 65. № 8. С. 564–572.

<https://doi.org/10.17073/0368-0797-2022-8-563-572>

INTRODUCTION

In recent times, materials science researchers have paid much attention to new high-entropy alloys (HEA) offering a range of unique properties [1–3]. The atoms of all elements in high-entropy alloys are considered dissolved matter atoms. They distort the lattice and improve the thermodynamic stability of the properties associated with the differences in atomic radii of the components. This leads to a high-entropy system suitable for making a material with unique properties which cannot be obtained through conventional microalloying.

The original HEA results are discussed in detail in reviews and monographs [4–7] presenting the HEA microstructure, properties, thermodynamics, structural simulation, and new multicomponent alloy manufacturing processes. The HEAs show that they may contain nanoscale structures and even amorphous phases due to the significant lattice distortions caused by the differences in the atomic radii of the substitution elements.

High-entropy FeCoCrNiMn alloy (Cantor) was one of the first to be studied. Its distinctive feature is that the lattice type (face-centered cubic) is not changed under a range of heat treatment modes. Furthermore, it has enhanced mechanical properties [8]. Mechanical tests of the alloy at cryogenic (77 K) and room temperatures indicated that its plastic deformation pattern is caused by the predominant twinning [9]. A disadvantage of CoCrFeMnNi alloys is their low yield strength at room temperature. It can be increased by microalloying, ultrasound treatment [10], nitriding [11], and boriding [12]. Such processes are challenging for industrial use since the elemental composition and the process variables need to be continuously monitored.

High-current electron-beam processing is one of the promising metal surface treatment processes. The ultra-fast heating and cooling of the surface significantly improve the mechanical properties by optimizing the surface layer structure [13]. The mechanical properties of metal parts after such treatment can be increased up to 20×. It is much higher than the for the conventional treatments [14, 15]. Low-energy, high-current electron beams also cause plastic deformation of the surface. This contributes to the formation of high-density dislocations and significantly improves the physical and mechanical properties [16, 17].

There are very few works studying the effects of low-energy high-current electron beam processing on high-entropy alloys. Lyu P. et al. [18] noted that the wear resistance, microhardness, nanohardness, and corrosion resistance of the CoCrFeNiMo_{0.2} alloy are significantly increased after electron-beam processing. It was shown that electron-beam processing homogenizes the chemical composition of the CoCrFeAlNi high-entropy alloy [19].

This study analyzes various methods for controlling the mechanical properties of Cantor high-entropy CoCrFeMnNi alloy.

RESULTS AND DISCUSSION

Alloying Effects

He J.Y. et al. [20] characterized and estimated the microstructure and tensile properties in several high-entropy alloys (FeCoNiCrMn)_{100-x}Al_x (x = 0 ÷ 20 at%) made with arc melting. Using the microstructural observations the phase diagram for the aluminum-containing alloys can be divided into three areas: a single HCC area, aluminum concentration below 8 % (area I); dup-

lex HCC + OCC phases, 8 to 16 % aluminum concentration (area II); an OCC solid solution area, over 16% aluminum concentration (area III). In area I ($Al < 8\%$), the alloys behave as solid solutions with aluminum atoms added as the primary strengthening element. The alloy's tensile strength is ~ 500 MPa, yield strength is ~ 220 MPa, and the relative elongation is 61.7 % to 47.2 %. In area II ($8\% < Al < 16\%$), the CCC phases can be found while the tensile strength and yield strength increase sharply, while ductility drops. The alloys in this area behave like a composite. For instance, 11 % aluminum HEA has a composite structure containing 25.4 % CCC. It features the max achievable tensile strength (1,174 MPa), and 7.7 % ductility. However, the alloys containing more than 11 % of aluminum have poor ductility. In area III ($Al > 16\%$), the alloys consist of disordered A2 segregations embedded in the ordered B2 matrix. The microstructural characterization suggests that the two OCC phases are a result of spinodal decomposition. The alloys in this area are extremely brittle.

Stepanov N.D. et al. [21] studied the microstructure and mechanical properties of high entropy CoCrFeMnNiV_x alloys ($x = 0; 0.25; 0.5; 0.75; 1.0$) produced by arc melting after their solidification and annealing at 1,000 °C for 24 h. A CoCrFeMnNi alloy is a single-phase HCC solid solution. The addition of vanadium leads to the formation of an intermetallic sigma phase in alloys where $x \geq 0.25$. The sigma phase was found in CoCrFeMnNiV_{0.5}, CoCrFeMnNiV_{0.75}, and CoCrFeMnNiV alloys after solidification and annealing. Annealing increases the sigma phase volume fraction in alloys with $x = 0.5, 0.75$, and 1.0, and also in the CoCrFeMnNiV_{0.25} alloy. The volume fraction of the sigma phase increases with vanadium content: from $\sim 2\%$ at $x = 0.25$ to 67 to 72 % at $x = 1.0$. The microhardness and yield strength measurements showed that adding vanadium above $x = 0.5$ increases the above values while reducing the ductility of the initially soft and ductile CoCrFeMnNi alloy. For example, the microhardness, yield strength, and ductility of the CoCrFeMnNi alloy are 135 HV, 230 MPa, and above 75 %, respectively. For the CoCrFeMnNiV alloy, they are 636 HV, 1,660 MPa, and 0.5 %, respectively.

Chen P. et al [22] proposed an unconventional alloying of HEA with manganese powder: by means of laser melting of the powder bed. In addition to its homogeneous dissolution in the HEA matrix, manganese also forms oxide particles (the oxygen comes both from the powder feedstock and the atmosphere). It produces in a HEA hardened with dispersed oxides. The result of this process is a HEA containing CoCrFeMnNi HCC matrix with $\sim 7\%$ volume fraction of manganese oxide particles.

High tensile strength (630/730 MPa yield strength/fracture strength) and moderate tensile ductility ($\sim 12\%$) were achieved by hardening with dispersed manganese oxide. The new HEA also retains high compressive ductility. HEA strength compared to CoCrFeMnNi made with a pre-alloyed powder is predominantly enhanced by the Orowan strengthening. The submicron oxide particles prevent plastic deformation of the matrix as they create voids along the sliding directions and to some extent reduce the tensile ductility.

Yamanaka S. et al. [23] studied the effects of titanium and silicon additions on the phase equilibrium and mechanical properties of the equiatomic, high-entropy CoCrFeMnNi alloy. It was found that the addition of both titanium and silicon improves tensile strength. The hardening capacity of the titanium addition is higher than that of silicon. The addition of titanium produces an alloy with lower ductility than the Cantor alloy. The difference in ductility is caused by strain hardening in the high strain range.

Xian X. et al. [24] studied the effects of adding copper at the phase transition and mechanical properties of the high-entropy CrMnFeCoNiCu_x alloy. Copper-depleted dendrites and copper- and manganese-rich interdendrites are observed in alloys with large copper content, due to the positive enthalpy of the copper mixing with other elements. The yield strength and microhardness increase with the copper content: from 188.04 to 350.63 MPa; and from 165.35 to 215.84 HV, respectively. The reason for the high strength of the CrMnFeCoNiCu alloy is the presence of nanoscale copper-rich particles uniformly dispersed across the matrix. They prevent the movement of dislocations as the alloy is deformed. Compression tests show that CrMnFeCoNiCu_x alloys with the addition of copper have an excellent strain hardening ability. Lu Y. et al. [25] processed high entropy Cantor-type alloys with carbon additions (0; 0.5 %; 2.0 at%) by twisting (0.5; 1; 3 turns) at 6.5 GPa and room temperature. For all the alloys studied, high plastic deformation leads to a sharp grain size refinement to the nanoscale and a significant increase in dislocation density. The hardness of the samples containing 0; 0.5; 2.0 at% of carbon approaches the max values of 490; 550; 640 HV, respectively. The relative elongation of the samples for all three alloys studied exceeds 30 %. The yield strength of the samples reaches 1.7; 1.9; 2.4 GPa at 0; 0.5; 2.0 at% carbon content, respectively but with a sharp ductility decrease. We analyzed the factors contributing to the hardening and identified that the conventional dislocation movement approach significantly overestimates the yield strength compared to the experimental values. It was assumed that the discrepancy

between the theoretical estimates and the experimental results is due to grain boundary sliding.

CoCrFeMnNi WEC composites [26] containing 2.5 wt% TiC and 5 wt% WC were obtained with laser melt deposition. The samples had a non-porous, compacted, two-phase microstructure of the HCC matrix and precipitates. Spherical precipitates of titanium carbide (TiC) ranging from 200 nm to more than 1 μm were observed in the samples with added TiC. Samples were found with added WC, 50 – 100 nm cubic Me_{23}C_6 precipitates. The HEA tensile strength was significantly improved by adding particles due to the combined effect of grain refinement and higher contribution of the precipitates. The ultimate tensile strength increased from 550 to 610 MPa, while ductility reduced from 52 to 47 % as 2.5 wt% of TiC was added. The mechanical properties of the samples with 5 wt% of WC added were as follows: 776 MPa ultimate tensile strength, and 37 % relative elongation. Zhang X. et al. [26] showed the potential of nanoscale TiC precipitations for controlling the HEA mechanical properties.

Ji W. et al. [27] used mechanical alloying and subsequent spark plasma sintering at 800 $^{\circ}\text{C}$ and 50 MPa to make an equiatomic HEA. Mechanical alloying forms a solid solution with a 10 nm fine microstructure consisting of HCC and OCC phases. After consolidation, only the HCC phase with high (1,987 MPa) compressive strength was found in the HEA. Spark plasma sintering induces an interesting magnetic transition associated with coarsening and phase transformation.

The nanostructure phase state was also achieved in the HEA alloy made by gas sputtering and subsequent powder hot pressing at 1,100 $^{\circ}\text{C}$ for 2 h [28]. Sintered equiatomic HEA is a homogeneous single-phase solid solution with the HCC structure and equiaxed grains (average size: $\sim 16 \mu\text{m}$). Transmission electron microscopy (TEM) studies showed that metastable structures ranging from 55 to 160 nm are created in the sintered metal. These structures are “inherited” from the gas-sputtered CoCrFeMnNi powder with nanoscale crystallites formed during rapid solidification. The yield strength at room temperature and the tensile strength of the sintered HEA reached 358 and 778 MPa, respectively, while the alloy retained excellent (about 28 %) ductility. EBSD studies of the substructures at certain strain levels showed that the sintered CoCrFeMnNi HEA retains a single-phase HCC structure, while the primary deformation pattern is dislocation sliding. The hardening is caused by a combined effect of grain refinement and the presence of nanoscale metastable structures.

Temperature and Microstructure Effects

The HEA mechanical properties depend on the test temperature and microstructure. Otto F. et al. [29] made an equiatomic high-entropy alloy by arc melting, injection molding, and rolling. Then the alloy was recrystallized to produce a single-phase HCC structure with three grain sizes: 4.4; 50; 155 μm . We studied the yield and tensile strength vs. temperature and grain size relationships in the 77 – 1,073 K temperature range.

Up to 873 K, the yield strength increased as the grain size decreased. The greatest increase occurred when the grain size decreased from 155 to 4.4 μm . The tensile strength also increased as the grain size decreased, although to a lesser extent than the yield strength. The elongation at break is comparable for samples with grain sizes of 50 and 155 μm and lower for finer-grained material. In the case of samples with grains of all three sizes (4.4, 50, and 155 μm), the alloy shows a strong increase in yield strength and ultimate tensile strength with decreasing temperature. Relative elongation at break also increased monotonically as the temperature decreased for the samples with 50 and 155 μm grain sizes. An intermediate temperature minimum of around 673 K for the fine-grained material was found.

In the 77 – 873 K temperature range, the initial plasticity up to the ~ 2 % tensile strain is caused exclusively by planar $1/2 \ 110$ dislocation glide along the $\{111\}$ slip plane. As the test temperature decreased from room temperature to 77 K, nanoscale twinning was observed as an additional mode of deformation. It probably contributes to the observed increase in ductility at low temperatures. In pure HCC metals, the yield strength increase with the temperature decrease found for this highly entropic HEA is rarely observed. Such yield strength increase in binary HCC solid solutions varies depending on the dissolved matter concentration. So far, TEM studies have not explained the temperature dependence of the yield strength. Note that the terms “dissolved matter” and “solvent” lose their usual meanings [29] when applied to thermally activated microstructural processes affecting the fluidity of equiatomic high-entropy alloys.

Severe Plastic Deformation and Impact Loading

The CoCrFeMnNi equiatomic high-entropy alloy produced by arc melting and drop casting was subjected to severe plastic deformation (SPD): high-pressure torsion [30]. It caused significant grain refinement to 50 nm

in the coarse casting part. The strength and the hardness were significantly increased: to 1,950 MPa and ~520 HV, respectively. After SPD, the alloy is still a single-phase solid solution down to the atomic scale. We performed isochronal (1 h) and isothermal heat treatment followed by microhardness and tensile tests. The isochronous annealing resulted in a significant hardness increase to 630 HV at 450 °C. Further temperature increase led to a decrease in hardness. The isothermal annealing at 450 °C caused an extra hardness increase to 910 HV after 100 h. In order to explain the unexpected response to annealing, we used a comprehensive microstructural analysis with TEM and 3D atom probe tomography. The formation of new nanophases in the initially single-phase HEA was detected. After very short anneals (5 min at 450 °C), the NiMn and chromium-rich phases were formed. As the annealing time increased, their volume fraction also increased, and a third FeCo phase was formed. The excess grain boundaries in a nanocrystalline HEA create multiple paths for rapid diffusion and nucleation sites to facilitate this phase decomposition. The increase in hardness, especially with longer annealing, may be explained by the presence of nanoscale phases within the HEA matrix.

Our results provide some valuable new insights into the phase stability of single-phase high-entropy alloys and the mechanical property control options.

Yim D. et al. [31] pressed mechanically alloyed powders of a high entropy alloy by static and shock-wave compaction followed by sintering without any pressure applied. It was shown that the alloy consists of the HCC phase with a small amount of ZrO₂ oxide after refinement and sintering. The presence of ZrO₂ oxide is associated with grinding contamination which led to the composite microstructure formation. Static compaction of alloyed powders increases the compaction density (~85–88 %) as the pressure increases (1–3 GPa), while shock wave compaction leads to a high (~95 %) relative density with fine, isolated pores. After sintering, the samples compacted by shock waves featured virtually complete (99.5 %) compaction with smaller grain size and better mechanical properties when compared to the sintering of statically compacted samples. A sintered sample compacted by a shock wave showed a high (630 MPa) yield strength and uniform strain distribution.

Electron-Beam Processing

The CoCrFeMnNi non-equiatomc high-entropy alloy was produced by means of wire-arc additive manufacturing (WAAM) [7]. We plotted and analyzed the HEA tensile strain curves in their initial state and after electron-

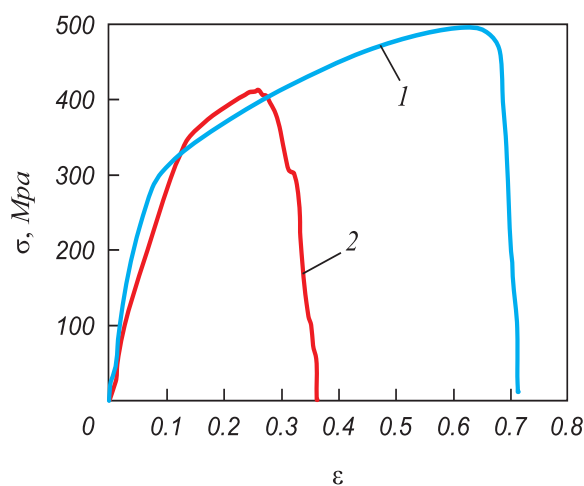
beam processing. The process variables were as follows: electron beam energy density $E_s = 10 - 30 \text{ J/cm}^2$; 50 μs duration; 3 pulses; and 0.3 s^{-1} pulse rate.

Our mechanical tests of the HEA in its initial and electron-beam processed states (uniaxial tension of flat proportional samples) showed that in its initial state (before processing), the alloy has high ductility (the relative elongation exceeds 70 %) and strength (the ultimate strength reaches 500 MPa) (see Fig., curve 1). Processing with a pulsed electron beam (high-speed melting and subsequent high-speed crystallization) of the surface layer reduces the strength and ductility (see Fig., curve 2).

The HEA electron-beam processing reduces the microhardness of the processed layer by $1.6\times$ (from 3.1 to 1.85 GPa at $E_s = 30 \text{ J/cm}^2$). Significant strength and plastic property changes are caused by the changes in the alloy's defective substructure initiated by the thermal impact of the electron beam.

We applied a pulsed electron beam with various energy densities to the HEA surface, in order to study the evolution of the defect substructure formed through high-speed heating and cooling. Electron-beam processing at $E_s = 10 \text{ J/cm}^2$ is accompanied by primary recrystallization of the surface layer.

At higher electron beam energy density (15–30 J/cm^2) collective recrystallization occurs in the surface layer, and the grain size grows. The average grain size increases from 35 to 120 μm as the electron beam energy density rises from 15 to 30 J/cm^2 .



Deformation curves for the HEA tension in its initial state (1) and after pulsed electron-beam processing (2) at $E_s = 30 \text{ J/cm}^2$

Деформационные кривые, полученные при растяжении ВЭС в исходном состоянии (1) и после облучения импульсным электронным пучком (2) при $E_s = 30 \text{ Дж/см}^2$

The scanning and transmission electron microscopy analysis of the processed surface and thin surface layer showed that the high-speed thermal impact forms a cellular crystallization structure in the surface layer. The average size of the crystallization cells depends on the electron beam energy density. It increases from 310 nm at $E_s = 15 \text{ J/cm}^2$ to 800 nm at $E_s = 30 \text{ J/cm}^2$.

Analysis of the uniaxial tension fracture surface showed that the cellular structure surface layer thickness is approximately 5 μm . The cells are nearly equiaxed in shape and form a columnar structure. It should be noted that the high-speed crystallization structure results in the formation of a micropore layer along the interface between the modified layer and the metal volume. We detected microcracks in the modified layer and the adjacent volume. The formation of such a defective substructure may be one of the reasons for the decrease in HEA strength and plastic properties after electron-beam processing.

See the table for a comparative analysis of the CoCrFeMnNi mechanical properties.

The significant differences detected may be explained by the shape and size of the samples, their manufacturing process, and test conditions.

CONCLUSIONS

The Cantor CoCrFeMnNi HCC HEA developed in 2004 offers a good combination of strength and ductility in a wide temperature range. It also has relatively low yield strength at room temperature. We reviewed the studies on changing the mechanical properties of the CoCrFeMnNi (equiatomic and non-equiatomic) HEAs by changing the manufacturing process. We also studied the effect of aluminum, vanadium, manganese, titanium, silicon, carbon, and copper alloying on the deformation hardening and other properties. We observed the effects of the 4.4 – 155 μm grain size and microstructure on the ultimate tensile strength and yield strength in a wide temperature range (77 – 1073 K). It was found that adding TiC and WC (2.5 wt% and 5.0 wt%) significantly increases the ultimate strength but reduces the relative

Comparative analysis of the mechanical properties for the CoCrFeMnNi alloys obtained by various processes

Сравнительный анализ механических свойств высокоэнтропийного сплава системы CoCrFeMnNi, полученного различными методами

Manufacturing process	Test type	Offset yield strength, MPa	Tensile strength, MPa	Relative strain, %	Microhardness, HV
This study	Compression	279	1689	54	153
	Tensile load	279	499	63	
Casting [20]	Compression	208	–	75	144
Casting [21]	Tensile load	230	–	62	176
Selective laser melting [22]	Tensile load	624	747	12.3	–
Laser metal deposition [26]	Tensile load	245	550	52	–
Arc melting, cold rolling + annealing at 800 °C [29]	Tensile load	350	670	–	–
Arc melting, cold rolling + annealing at 1000 °C [29]	Tensile load	180	580	–	–
Arc melting, cold rolling + annealing at 1150 °C [29]	Tensile load	160	530	–	–
Severe plastic deformation [30]	Tensile load	1900	1950	–	–
Mechanical alloying and plasma sintering [27]	Tensile load	1760	1950	–	–
Mechanical alloying and shock sintering (1 h) [31]	Tensile load	630	800	–	–
Powder gas sputtering hot pressing [28]	Tensile load	358	778	–	–

elongation at break. Severe plastic deformation increases the tensile strength to 1,950 MPa and hardness to 520 HV by forming a nanoscale (~50 nm) grain structure. The mechanical properties can be changed by subsequent isochoric and isothermal annealing. The nanostructure phase states created by impact compacting, mechanical alloying and subsequent plasma sintering significantly increase the ultimate strength, while maintaining high

ductility (28 % relative elongation). We analyzed the deformation curves for the non-equiatomic HEAs made by wire-arc additive manufacturing technology with subsequent electron-beam processing, and explained the decrease in strength and plastic properties. We also proposed reasons why the mechanical properties of the Cantor CoCrFeMnNi HEA obtained by different processes are different.

REFERENCES

СПИСОК ЛИТЕРАТУРЫ

- George E.P., Curtin W.A., Tazan C.C. High entropy alloys: A focused review of mechanical properties and deformation mechanisms. *Acta Materialia*. 2020, vol. 188, pp. 435–474. <https://doi.org/10.1016/j.actamat.2019.12.015>
- Shivam V., Basu J., Pandey V.K., Shadangi Y., Mukhopadhyay N.K. Alloying behaviour, thermal stability and phase evolution in quinary AlCoCrFeNi high entropy alloy. *Advanced Powder Technology*. 2018, vol. 29, no. 9, pp. 2221–2230. <https://doi.org/10.1016/j.appt.2018.06.006>
- Ganesh U.L., Raghavendra H. Review on the transition from conventional to multi-component-based nano-high-entropy alloys-NHEAs. *Journal of Thermal Analysis and Calorimetry*. 2020, vol. 139, pp. 207–216. <https://doi.org/10.1007/s10973-019-08360-z>
- Miracle D.B., Senkov O.N. A critical review of high entropy alloys and related concepts. *Acta Materialia*. 2017, vol. 122, pp. 448–511. <https://doi.org/10.1016/j.actamat.2016.08.081>
- Zhang W., Liaw P.K., Zhang Y. Science and technology in high-entropy alloys. *Science China Materials*. 2018, vol. 61, no. 1, pp. 2–22. <https://doi.org/10.1007/s40843-017-9195-8>
- Osintsev K.A., Gromov V.E., Kononov S.V., Ivanov Yu.F., Panchenko I.A. High-entropy alloys: Structure, mechanical properties, deformation mechanisms and application. *Izvestiya. Ferrous Metallurgy*. 2021, vol. 64, no. 4, pp. 249–258. (In Russ.). <https://doi.org/10.17073/0368-0797-2021-4-249-258>
- Gromov V.E., Kononov S.V., Ivanov Yu.F., Osintsev K.A. High-entropy alloys of AlCoCrFeNi-system. *Advanced Structured Materials*, 2021, vol. 107, pp. 79–110. https://doi.org/10.1007/978-3-030-78364-8_6
- Zhang T., Xin L., Wu F., Zhao R., Xiang J., Chen M., Jiang S., Huang Y., Chen S. Microstructure and mechanical of Fe_xCoCrNiMn high-entropy alloys. *Journal of Materials Science and Technology*. 2019, vol. 35, no. 10, pp. 2331–2335. <https://doi.org/10.1016/j.jmst.2019.05.050>
- Gludovatz B.A., Hohenwarter A., Catoor D., Chang E.H., George E.P., Ritchie R.O. Fracture-resistant high-entropy alloy for cryogenic applications. *Science*. 2014, vol. 345, no. 6201, pp. 1153–1158. <https://doi.org/10.1126/science.1254581>
- Listyawan T.A., Lee H., Park N., Lee U. Microstructure and mechanical properties of CoCrFeMnNi high entropy alloy with ultrasonic nanocrystal modification process. *Journal of Materials Science and Technology*. 2020, vol. 57, pp. 123–130. <https://doi.org/10.1016/j.jmst.2020.02.083>
- Meng F., Baker I. Nitriding of a high entropy FeNiMnAlCr alloy. *Journal of Alloys and Compounds*. 2015, vol. 645, pp. 376–381. <https://doi.org/10.1016/j.jallcom.2015.05.021>
- Lindner T., Löbel M., Sattler B., Lampke T. Surface hardening of FCC phase high-entropy alloy system by powder-pack boriding. *Surface and Coatings Technology*. 2019, vol. 371, pp. 389–394. <https://doi.org/10.1016/j.surfcoat.2018.10.017>
- George E.P., Curtin W.A., Tazan C.C. High entropy alloys: A focused review of mechanical properties and deformation mechanisms // *Acta Materialia*. 2020. Vol. 188. P. 435–474. <https://doi.org/10.1016/j.actamat.2019.12.015>
- Shivam V., Basu J., Pandey V.K., Shadangi Y., Mukhopadhyay N.K. Alloying behaviour, thermal stability and phase evolution in quinary AlCoCrFeNi high entropy alloy // *Advanced Powder Technology*. 2018. Vol. 29. No. 9. P. 2221–2230. <https://doi.org/10.1016/j.appt.2018.06.006>
- Ganesh U.L., Raghavendra H. Review on the transition from conventional to multi-component-based nano-high-entropy alloys-NHEAs // *Journal of Thermal Analysis and Calorimetry*. 2020. Vol. 139. P. 207–216. <https://doi.org/10.1007/s10973-019-08360-z>
- Miracle D.B., Senkov O.N. A critical review of high entropy alloys and related concepts // *Acta Materialia*. 2017. Vol. 122. P. 448–511. <https://doi.org/10.1016/j.actamat.2016.08.081>
- Zhang W., Liaw P.K., Zhang Y. Science and technology in high-entropy alloys // *Science China Materials*. 2018. Vol. 61. No. 1. P. 2–22. <https://doi.org/10.1007/s40843-017-9195-8>
- Осинцев К.А., Громов В.Е., Кононов С.В., Иванов Ю.Ф., Панченко И.А. Высокоэнтропийные сплавы: структура, механические свойства, механизмы деформации и применение // *Известия вузов. Черная металлургия*. 2021. Т. 64. № 4. С. 249–258. <https://doi.org/10.17073/0368-0797-2021-4-249-258>
- Gromov V.E., Kononov S.V., Ivanov Yu.F., Osintsev K.A. High-entropy alloys of AlCoCrFeNi-system // *Advanced Structured Materials*. 2021. Vol. 107. P. 79–110. https://doi.org/10.1007/978-3-030-78364-8_6
- Zhang T., Xin L., Wu F., Zhao R., Xiang J., Chen M., Jiang S., Huang Y., Chen S. Microstructure and mechanical of Fe_xCoCrNiMn high-entropy alloys // *Journal of Materials Science and Technology*. 2019. Vol. 35. No. 10. P. 2331–2335. <https://doi.org/10.1016/j.jmst.2019.05.050>
- Gludovatz B.A., Hohenwarter A., Catoor D., Chang E.H., George E.P., Ritchie R.O. Fracture-resistant high-entropy alloy for cryogenic applications // *Science*. 2014. Vol. 345. No. 6201. P. 1153–1158. <https://doi.org/10.1126/science.1254581>
- Listyawan T.A., Lee H., Park N., Lee U. Microstructure and mechanical properties of CoCrFeMnNi high entropy alloy with ultrasonic nanocrystal modification process // *Journal of Materials Science and Technology*. 2020. Vol. 57. P. 123–130. <https://doi.org/10.1016/j.jmst.2020.02.083>
- Meng F., Baker I. Nitriding of a high entropy FeNiMnAlCr alloy // *Journal of Alloys and Compounds*. 2015. Vol. 645. P. 376–381. <https://doi.org/10.1016/j.jallcom.2015.05.021>
- Lindner T., Löbel M., Sattler B., Lampke T. Surface hardening of FCC phase high-entropy alloy system by powder-pack boriding // *Surface and Coatings Technology*. 2019. Vol. 371. P. 389–394. <https://doi.org/10.1016/j.surfcoat.2018.10.017>

13. Proskiyrovsky D.I., Rotshtein V.P., Ozur G.E., Ivanov Yu.F., Markov A.B. Physical foundations for surface treatment of materials with low energy, high current electron beams. *Surface and Coatings Technology*. 2000, vol. 125, no. 1-3, pp. 49–56.
[https://doi.org/10.1016/S0257-8972\(99\)00604-0](https://doi.org/10.1016/S0257-8972(99)00604-0)
14. Valkov S., Ormanova M., Petrov P. Electron-beam surface treatment of metals and alloys: Techniques and trends. *Metals*. 2020, vol. 10, no. 9, article 10091219. <https://doi.org/10.3390/met10091219>
15. Konovalov S., Ivanov Y., Gromov V., Panchenko I. Fatigue-induced evolution of AISI 310S steel microstructure after electron beam treatment. *Materials*. 2020, vol. 13, no. 20, article 4567.
<https://doi.org/10.3390/ma13204567>
16. Zhang C., Lv P., Xia H., Yang Z., Konovalov S., Chen X., Guan Q. The microstructure and properties of nanostructured Cr-Al alloying layer fabricated high-current pulsed electron beam. *Vacuum*. 2019, vol. 167, pp. 263–270. <https://doi.org/10.1016/j.vacuum.2019.06.022>
17. Konovalov S.V., Komissarova I.A., Kosinov D.A., Ivanov Yu.F., Ivanova O.V., Gromov V.E. Structure of titanium alloy, modified by electron beams and destroyed during fatigue. *Letters on Materials*. 2017, vol. 7, no. 3, pp. 266–271.
<https://doi.org/10.22226/2410-3535-2017-3-266-271>
18. Lyu P., Peng T., Miao Y., Liu Z., Gao Q., Zhang C., Jin Y., Guan Q., Cai J. Microstructure and properties of CoCrFeNiMo_{0.2} high-entropy alloy enhanced by high-current pulsed electron beam. *Surface and Coatings Technology*. 2021, vol. 410, article 126911.
<https://doi.org/10.1016/j.surfcoat.2021.126911>
19. Osintsev K., Gromov V., Ivanov Y., Konovalov S., Panchenko I., Vorobyev S. Evolution of structure in AlCoCrFeNi high-entropy alloy irradiated by a pulsed electron beam. *Metals*. 2021, vol. 11, no. 8, article 1228. <https://doi.org/10.3390/met11081228>
20. He J.Y., Liu W.H., Wang H., Wu Y., Liu X.J., Nieh T.G., Lu Z.P. Effects of Al addition on structural evolution and tensile properties of the FeCoNiCrMn high-entropy alloy system. *Acta Materialia*. 2014, vol. 62, pp. 105–113.
<https://doi.org/10.1016/j.actamat.2013.09.037>
21. Stepanov N.D., Shaysultanov D.G., Salishchev G.A., Tikhonovskiy M.A., Oleynik E.E., Tortika A.S., Senkov O.N. Effect of V content on microstructure and mechanical properties of the CoCrFeMnNiV_x high entropy alloys. *Journal of Alloys and Compounds*. 2015, vol. 628, pp. 170–185.
<https://doi.org/10.1016/j.jallcom.2014.12.157>
22. Chen P., Yang C., Li S., Attallah M.M., Yan M. In-situ alloyed, oxide-dispersion-strengthened CoCrFeMnNi high entropy alloy fabricated via laser powder bed fusion. *Materials & Design*. 2020, vol. 194, article 108966. <https://doi.org/10.1016/j.matdes.2020.108966>
23. Yamanaka S., Ikeda K-i., Miura S. The effect of titanium and silicon addition on phase equilibrium and mechanical properties of CoCrFeMnNi-based high entropy alloy. *Journal of Materials Research*. 2021, vol. 36, no. 10, pp. 2056–2070.
<https://doi.org/10.1557/s43578-021-00251-0>
24. Xian X., Lin L., Zhong Z., Zhang C., Chen C., Song K., Cheng J., Wu Y. Precipitation and its strengthening of Cu-rich phase in CrMnFeCoNiCu_x high-entropy alloys. *Materials Science and Engineering: A*. 2018, vol. 713, pp. 134–140.
<https://doi.org/10.1016/j.msea.2017.12.060>
25. Lu Y., Mazilkin A., Boll T., Stepanov N., Zharebtzov S., Salishchev G., Ódore É., Ungar T., Lavernia E., Hahn H., Ivanisenko Y. Influence of carbon on the mechanical behavior and microstructure evolution of CoCrFeMnNi processed by high pressure torsion. *Materialia*. 2021, vol. 16, article 101059.
<https://doi.org/10.1016/j.mtla.2021.101059>
13. Proskiyrovsky D.I., Rotshtein V.P., Ozur G.E., Ivanov Yu.F., Markov A.B. Physical foundations for surface treatment of materials with low energy, high current electron beams // *Surface and Coatings Technology*. 2000. Vol. 125. No. 1-3. P. 49–56.
[https://doi.org/10.1016/S0257-8972\(99\)00604-0](https://doi.org/10.1016/S0257-8972(99)00604-0)
14. Valkov S., Ormanova M., Petrov P. Electron-beam surface treatment of metals and alloys: Techniques and trends // *Metals*. 2020. Vol. 10. No. 9. Article 10091219. <https://doi.org/10.3390/met10091219>
15. Konovalov S., Ivanov Y., Gromov V., Panchenko I. Fatigue-induced evolution of AISI 310S steel microstructure after electron beam treatment // *Materials*. 2020. Vol. 13. No. 20. Article 4567.
<https://doi.org/10.3390/ma13204567>
16. Zhang C., Lv P., Xia H., Yang Z., Konovalov S., Chen X., Guan Q. The microstructure and properties of nanostructured Cr-Al alloying layer fabricated high-current pulsed electron beam // *Vacuum*. 2019. Vol. 167. P. 263–270. <https://doi.org/10.1016/j.vacuum.2019.06.022>
17. Konovalov S.V., Komissarova I.A., Kosinov D.A., Ivanov Yu.F., Ivanova O.V., Gromov V.E. Structure of titanium alloy, modified by electron beams and destroyed during fatigue // *Letters on Materials*. 2017. Vol. 7. No. 3. P. 266–271.
<https://doi.org/10.22226/2410-3535-2017-3-266-271>
18. Lyu P., Peng T., Miao Y., Liu Z., Gao Q., Zhang C., Jin Y., Guan Q., Cai J. Microstructure and properties of CoCrFeNiMo_{0.2} high-entropy alloy enhanced by high-current pulsed electron beam // *Surface and Coatings Technology*. 2021. Vol. 410. Article 126911.
<https://doi.org/10.1016/j.surfcoat.2021.126911>
19. Osintsev K., Gromov V., Ivanov Y., Konovalov S., Panchenko I., Vorobyev S. Evolution of structure in AlCoCrFeNi high-entropy alloy irradiated by a pulsed electron beam // *Metals*. 2021. Vol. 11. No. 8. Article 1228. <https://doi.org/10.3390/met11081228>
20. He J.Y., Liu W.H., Wang H., Wu Y., Liu X.J., Nieh T.G., Lu Z.P. Effects of Al addition on structural evolution and tensile properties of the FeCoNiCrMn high-entropy alloy system // *Acta Materialia*. 2014. Vol. 62. P. 105–113.
<https://doi.org/10.1016/j.actamat.2013.09.037>
21. Stepanov N.D., Shaysultanov D.G., Salishchev G.A., Tikhonovskiy M.A., Oleynik E.E., Tortika A.S., Senkov O.N. Effect of V content on microstructure and mechanical properties of the CoCrFeMnNiV_x high entropy alloys // *Journal of Alloys and Compounds*. 2015. Vol. 628. P. 170–185.
<https://doi.org/10.1016/j.jallcom.2014.12.157>
22. Chen P., Yang C., Li S., Attallah M.M., Yan M. In-situ alloyed, oxide-dispersion-strengthened CoCrFeMnNi high entropy alloy fabricated via laser powder bed fusion // *Materials & Design*. 2020. Vol. 194. Article 108966. <https://doi.org/10.1016/j.matdes.2020.108966>
23. Yamanaka S., Ikeda K-i., Miura S. The effect of titanium and silicon addition on phase equilibrium and mechanical properties of CoCrFeMnNi-based high entropy alloy // *Journal of Materials Research*. 2021. Vol. 36. No. 10. P. 2056–2070.
<https://doi.org/10.1557/s43578-021-00251-0>
24. Xian X., Lin L., Zhong Z., Zhang C., Chen C., Song K., Cheng J., Wu Y. Precipitation and its strengthening of Cu-rich phase in CrMnFeCoNiCu_x high-entropy alloys // *Materials Science and Engineering: A*. 2018. Vol. 713. P. 134–140.
<https://doi.org/10.1016/j.msea.2017.12.060>
25. Lu Y., Mazilkin A., Boll T., Stepanov N., Zharebtzov S., Salishchev G., Ódore É., Ungar T., Lavernia E., Hahn H., Ivanisenko Y. Influence of carbon on the mechanical behavior and microstructure evolution of CoCrFeMnNi processed by high pressure torsion // *Materialia*. 2021. Vol. 16. Article 101059.
<https://doi.org/10.1016/j.mtla.2021.101059>

26. Zhang X., Li R., Huang L., Amar A., Wu C., Le G., Liu X., Guan D., Yang G., Li J. Influence of in-situ and ex-situ precipitations on microstructure and mechanical properties of additive manufacturing CoCrFeMnNi high-entropy alloys. *Vacuum*. 2021, vol. 187, article 110111. <https://doi.org/10.1016/j.vacuum.2021.110111>
27. Ji W., Wang W., Wang H., Zhang J., Wang Y., Zhang F., Fu Z. Alloying behavior and novel properties of CoCrFeNiMn high-entropy alloy fabricated by mechanical alloying and spark plasma sintering. *Intermetallics*. 2015, vol. 56, pp. 24–27. <https://doi.org/10.1016/j.intermet.2014.08.008>
28. Yang T., Cai B., Shi Y., Wang M., Zhang G. Preparation of nanostructured CoCrFeMnNi high entropy alloy by hot pressing sintering gas atomized powders. *Micron*. 2021, vol. 147, pp. article 103082. <https://doi.org/10.1016/j.micron.2021.103082>
29. Otto F., Dlouhý A., Somsen Ch., Bei H., Eggeler G., George E.P. The influences of temperature and microstructure on the tensile properties of a CoCrFeMnNi high-entropy alloy. *Acta Materialia*. 2013, vol. 61, no. 15, pp. 5743–5755. <https://doi.org/10.1016/j.actamat.2013.06.018>
30. Schuh B., Mendez-Martin F., Völker B., George E.P., Clemens H., Pippin R., Hohenwarter A. Mechanical properties, microstructure and thermal stability of a nanocrystalline CoCrFeMnNi high-entropy alloy after severe plastic deformation. *Acta Materialia*. 2015, vol. 96, pp. 258–268. <https://doi.org/10.1016/j.actamat.2015.06.025>
31. Yim D., Kim W., Praveen S., Jang M.J., Bae J.W., Moon J., Kim E., Hong S.-J., Kim H.S. Shock wave compaction and sintering of mechanically alloyed CoCrFeMnNi high-entropy alloy powders. *Materials Science and Engineering: A*. 2017, vol. 708, pp. 291–300. <https://doi.org/10.1016/j.msea.2017.09.132>
26. Zhang X., Li R., Huang L., Amar A., Wu C., Le G., Liu X., Guan D., Yang G., Li J. Influence of in-situ and ex-situ precipitations on microstructure and mechanical properties of additive manufacturing CoCrFeMnNi high-entropy alloys // *Vacuum*. 2021. Vol. 187. Article 110111. <https://doi.org/10.1016/j.vacuum.2021.110111>
27. Ji W., Wang W., Wang H., Zhang J., Wang Y., Zhang F., Fu Z. Alloying behavior and novel properties of CoCrFeNiMn high-entropy alloy fabricated by mechanical alloying and spark plasma sintering // *Intermetallics*. 2015. Vol. 56. P. 24–27. <https://doi.org/10.1016/j.intermet.2014.08.008>
28. Yang T., Cai B., Shi Y., Wang M., Zhang G. Preparation of nanostructured CoCrFeMnNi high entropy alloy by hot pressing sintering gas atomized powders // *Micron*. 2021. Vol. 147. Article 103082. <https://doi.org/10.1016/j.micron.2021.103082>
29. Otto F., Dlouhý A., Somsen Ch., Bei H., Eggeler G., George E.P. The influences of temperature and microstructure on the tensile properties of a CoCrFeMnNi high-entropy alloy // *Acta Materialia*. 2013. Vol. 61. No. 15. P. 5743–5755. <https://doi.org/10.1016/j.actamat.2013.06.018>
30. Schuh B., Mendez-Martin F., Völker B., George E.P., Clemens H., Pippin R., Hohenwarter A. Mechanical properties, microstructure and thermal stability of a nanocrystalline CoCrFeMnNi high-entropy alloy after severe plastic deformation // *Acta Materialia*. 2015. Vol. 96. P. 258–268. <https://doi.org/10.1016/j.actamat.2015.06.025>
31. Yim D., Kim W., Praveen S., Jang M.J., Bae J.W., Moon J., Kim E., Hong S.-J., Kim H.S. Shock wave compaction and sintering of mechanically alloyed CoCrFeMnNi high-entropy alloy powders // *Materials Science and Engineering: A*. 2017. Vol. 708. P. 291–300. <https://doi.org/10.1016/j.msea.2017.09.132>

INFORMATION ABOUT THE AUTHORS

СВЕДЕНИЯ ОБ АВТОРАХ

Viktor E. Gromov, Dr. Sci. (Phys.-Math.), Prof., Head of the Chair of Science named after V.M. Finkel', Siberian State Industrial University
ORCID: 0000-0002-5147-5343
E-mail: gromov@physics.sibsiu.ru

Sergei V. Kononov, Dr. Sci. (Eng.), Prof., Head of the Chair of Metals Technology and Aviation Materials, Samara National Research University; Chief Researcher of Department of Scientific Researches, Siberian State Industrial University
ORCID: 0000-0003-4809-8660
E-mail: kononov@sibsiu.ru

Yuliya A. Shlyarova, Postgraduate of the Chair of Science named after V.M. Finkel', Research Associate of the Laboratory of Electron Microscopy and Image Processing, Siberian State Industrial University
ORCID: 0000-0001-5677-1427
E-mail: rubannikova96@mail.ru

Michail O. Efimov, Engineer of Department of Scientific Research, Siberian State Industrial University
E-mail: moefimov@mail.ru

Irina A. Panchenko, Cand. Sci. (Eng.), Head of the Laboratory of Electron Microscopy and Image Processing, Siberian State Industrial University
ORCID: 0000-0002-1631-9644
E-mail: i.i.ss@yandex.ru

Виктор Евгеньевич Громов, д.ф.-м.н., профессор, заведующий кафедрой естественнонаучных дисциплин им. профессора В.М. Финкеля, Сибирский государственный индустриальный университет
ORCID: 0000-0002-5147-5343
E-mail: gromov@physics.sibsiu.ru

Сергей Валерьевич Кононов, д.т.н., профессор, заведующий кафедрой технологии металлов и авиационного материаловедения, Самарский национальный исследовательский университет им. академика С.П. Королева; главный научный сотрудник Управления научных исследований, Сибирский государственный индустриальный университет
ORCID: 0000-0003-4809-8660
E-mail: kononov@sibsiu.ru

Юлия Андреевна Шлярова, аспирант кафедры естественнонаучных дисциплин им. профессора В.М. Финкеля, научный сотрудник лаборатории электронной микроскопии и обработки изображений, Сибирский государственный индустриальный университет
ORCID: 0000-0001-5677-1427
E-mail: rubannikova96@mail.ru

Михаил Олегович Ефимов, инженер Управления научных исследований, Сибирский государственный индустриальный университет
E-mail: moefimov@mail.ru

Ирина Алексеевна Панченко, к.т.н. заведующий лабораторией электронной микроскопии и обработки изображений, Сибирский государственный индустриальный университет
ORCID: 0000-0002-1631-9644
E-mail: i.i.ss@yandex.ru

CONTRIBUTION OF THE AUTHORS

ВКЛАД АВТОРОВ

V. E. Gromov – formation of the article concept, analysis of various ways to improve the mechanical properties of Cantor HEA, writing the article first version.

S. V. Kononov – analysis of the data on change in mechanical properties of HEA due to various methods of its production.

Yu. A. Shlyarova – selection of English-language literature on possible ways to improve the mechanical properties of the Cantor HEA in recent years.

M. O. Efimov – analysis of the work of foreign researchers on the influence of temperature and structure on HEA mechanical properties.

I. A. Panchenko – analysis of the work of foreign researchers on the effect of alloying on HEA properties.

В. Е. Громов – формирование концепции статьи, анализ различных способов улучшения механических свойств ВЭС Cantor; написание первого варианта статьи.

С. В. Коновалов – анализ данных по изменению механических свойств ВЭС за счет различных методов его получения.

Ю. А. Шлярова – подбор англоязычной литературы по возможным способам улучшения механических свойств ВЭС Cantor за последние годы.

М. О. Ефимов – анализ работ зарубежных исследователей по влиянию температуры и микроструктуры на механические свойства ВЭС.

И. А. Панченко – анализ работ зарубежных исследователей по влиянию легирования на свойства ВЭС.

Received 21.02.2022

Revised 03.03.2022

Accepted 11.03.2022

Поступила в редакцию 21.02.2022

После доработки 03.03.2022

Принята к публикации 11.03.2022